Available online at www.sciencedirect.com

ScienceDirect

Advances in Space Research 47 (2011) 1558–1567

ADVANCES IN SPACE RESEARCH (a COSPAR publication)

www.elsevier.com/locate/asr

Ion- and electron-acoustic solitons and double layers in multi-component space plasmas

G.S. Lakhina *, S.V. Singh, A.P. Kakad

Indian Institute of Geomagnetism, New Panvel (West), Navi Mumbai 410 218, India

Received 10 September 2010; received in revised form 10 December 2010; accepted 14 December 2010
Available online 22 December 2010

Abstract

A general model for the ion- and electron-acoustic solitons and double layers in a multi-component unmagnetized plasma consisting of background electrons, counter-streaming electron beams and ions is discussed. The model is based on the multi-fluid equations and the Poisson equation, and uses the Sagdeev pseudo-potential techniques. For identical counter-streaming electron beams and depending upon the plasma parameters, three types of solutions, namely, ion-acoustic, slow and fast electron-acoustic soliton/double layer, are possible. Generally, the ion acoustic solitons have positive potentials, slow-electron acoustic solitons have negative potentials and fast electron-acoustic solitons and double layers can have either positive or negative potentials depending on the core electron density. As beam speed is increased, first ion-acoustic and then slow electron-acoustic solitons disappear. At large beam speed, only fast electron-acoustic solitons/double layers survive. The results may be relevant to the observations of the electrostatic solitary waves (ESWs) observed in the Earth's magnetosphere.

Keywords: Electrostatic solitary waves; Solitons and double layers in space plasmas; Nonlinear ion- and electron-acoustic waves

1. Introduction

Electrostatic solitary waves (ESWs) have been observed in several regions of the Earth's magnetosphere, e.g., the bow shock (Bale et al., 1998), magnetosheath (Pickett et al., 2003, 2005), magnetopause and on cusp field lines (Franz et al., 1998; Cattell et al., 1999), Polar cap boundary layer (Tsurutani et al., 1998), auroral field lines (Temerin et al., 1982; Bostrom et al., 1988; Dubouloz et al., 1991a,b; Mozer et al., 1997; Ergun et al., 1998; Bounds et al., 1999), auroral kilometric radiation (AKR) source region (Pottelette et al., 1999), and plasma sheet boundary layer (PSBL) (Matsumoto et al., 1994; Omura et al., 1994, 1999). The ESWs are observed in the electric field component parallel to the background magnetic field, and are usually bipolar or some times tripolar. The ESWs are generally associated with electron or/and ion beams (Omura et al., 1994, 1999; Bounds et al., 1999; Singh, 2003). Further, the ESWs can have either positive or negative potentials. The electric field amplitude of ESWs can be a few mV/m in the PSBL to a few 100 mV/m in the dayside auroral zone. The velocities of ESWs can vary from $\sim$ a few hundred to a few thousand km s^{-1}, and their parallel scale sizes from $\sim$100 m to a few 1000 m.

The solitary waves with negative potentials observed by Viking satellite have been explained by various multi-component plasmas models (Pottelette et al., 1990; Mace et al., 1991; Dubouloz et al., 1991a, 1993; Singh et al., 2001a,b; Singh and Lakhina, 2004; Tagare et al., 2004). These models could not explain the positive potential solitary structures observed by Polar, FAST and Cluster. Berthomier et al. (2000, 2003) and El-Taibany (2005) studied the electron-acoustic solitons in four-component plasma and showed that, depending upon the beam velocity, temperature and density, solitons with positive polarity could be generated. For a detailed discussion of earlier models, one can refer to Lakhina et al. (2000, 2003).

* Corresponding author.
E-mail address: lakhina@iigs.iigm.res.in (G.S. Lakhina).

0273-1177/$36.00 © 2010 COSPAR. Published by Elsevier Ltd. All rights reserved.
doi:10.1016/j.asr.2010.12.013

Verheest et al. (2005) showed that positive potential electron-acoustic solitons can be generated even without the electron-beam component, provided the hot electron inertia is retained in the analysis. Kakad et al. (2009) discussed small amplitude electron-acoustic solitary waves in a plasma consisting of cold electrons and isothermal ions with two different temperatures. Their model supported the existence of solitons having either positive or negative potentials depending on the plasma parameters. Earlier, Kakad et al. (2007) showed that for some specific parametric range, the rarefactive and compressive electron-acoustic solitons can coexist in a four-component unmagnetized plasma system consisting of cold background electrons, a cold electron beam, and two types of ion species, cold and hot, both having Boltzmann distributions. Mamun et al. (2002) and Ghosh et al. (2008) studied the obliquely propagating electron-acoustic solitary waves in a magnetized multi-component plasma. They showed that the characteristics and existence domain of the positive potential solitons is controlled by the ion temperature and concentration.

Recently, Lakhina et al. (2008a) studied ion and electron acoustic solitary waves in a three-component plasma system consisting of cold and hot electrons and one type of ions. For a given set of plasma parameters, the critical Mach numbers for the ion-acoustic solitons were found to be smaller than those for electron-acoustic solitons. The ion-acoustic solitons had positive potentials whereas the electron-acoustic solitons could have positive (negative) potentials when the fractional cold electron density with respect to the ion density was greater (less) than a certain critical value. Introduction of a second ion species, i.e., a hot ion beam in the analysis lead to the existence of three types of solitary waves, namely, slow ion-acoustic, ion-acoustic and electron-acoustic solitons provided the Mach numbers exceed the respective critical values (Lakhina et al., 2008b).

More recently, Lakhina et al. (2009) developed a model for ion- and electron-acoustic solitons and double layers in a four-component plasma system consisting of core electrons, two counter-streaming electron beams and one type of ions. Actual plasma parameters corresponding to bipolar and tripolar pulses of ~25 to 100 μs durations observed by the Cluster spacecraft in the dayside magnetosheath (Pickett et al., 2005) were put into this model. Only one positive critical Mach number, M_0, apparently related to fast electron acoustic beam mode was found which yielded soliton and/or double layer solution. The estimates of the electric field, pulse duration and propagation speeds of the solitary structures predicted by the model were in good agreement with the observed bipolar pulses.

In addition to the magentosheath region, the counterstreaming electron beams have also been observed near the diffusion region of the magnetotail reconnection (Deng et al., 2006; Åsnes et al., 2008; Li et al., 2009), in the plasma sheet boundary layer (Parks et al., 1984; Teste and Parks, 2009; Pickett et al., 2009), dawn-flank plasma sheet (Fujimoto et al., 1997), and on the auroral field lines (Dubouloz et al., 1991a; McFadden et al., 1998). The electron beams, in each of these regions, have different properties. The purpose of this paper here is to undertake a detailed parametric study of Lakhina et al. (2009) model and investigate the effects of counterstreaming electron beam density and temperature, core electron density and temperature on the existence and nature of the solitons (i.e., ion-acoustic, slow and fast electron-acoustic) in these regions.

2. General soliton/double layer model

We consider a homogeneous, collisionless, and magnetized four component plasma consisting of core electrons (N_c, T_c, v_c), two electron beams (N_1, T_1, v_1) and (N_2, T_2, v_2) propagating along magnetic field, and ions (N_i, T_i, v_i), where N_j, T_j, v_j represents the equilibrium values of the density, temperature and beam velocity (along the direction of wave propagation) of the species j, and $j = i$, c, 1, and 2 for the ions, core electrons, beam 1 electrons and beam 2 electrons, respectively. We consider only the nonlinear electrostatic waves propagating parallel to the magnetic field, in which case the dynamics of the species is governed by the multi-fluid equations of continuity, momentum, and equation of state of each species, and the Poisson equation (Lakhina et al., 2009).

$$\frac{\partial n_j}{\partial t} + \frac{\partial (n_j v_j)}{\partial x} = 0, \tag{1}$$

$$\frac{\partial v_j}{\partial t} + v_j \frac{\partial v_j}{\partial x} + \frac{1}{\mu_j n_j} \frac{\partial P_j}{\partial x} - \frac{Z_j}{\mu_j} \frac{\partial \phi}{\partial x} = 0, \tag{2}$$

$$\frac{\partial P_j}{\partial t} + v_j \frac{\partial P_j}{\partial x} + 3P_j \frac{\partial v_j}{\partial x} = 0, \tag{3}$$

$$\frac{\partial^2 \phi}{\partial x^2} = n_c + n_1 + n_2 - n_i. \tag{4}$$

Here, $\mu_j = m_j/m_i$ (m_j and m_i represent the mass of the jth species and the ions, respectively) and $Z_j = +1\,(-1)$ for electrons (ions), respectively. Further, all densities are normalized with the unperturbed ion density, $N_i = N_c + N_1 + N_2$, velocities with the ion thermal velocity $C_i = (T_i/m_i)^{1/2}$, time with the inverse of ion plasma frequency, $\omega_{pi} = (4\pi N_i e^2/m_i)^{1/2}$, the lengths with the ion Debye length, $\lambda_{di} = (T_i/4\pi N_i e^2)^{1/2}$, the electrostatic potential ϕ by T_i/e, and the thermal pressures P_j with $N_i T_i$. Furthermore, we have assumed the same adiabatic index, i.e., $\gamma = 3$, for all the species in the equation of state given by Eq. (3).

In order to study the properties of arbitrary amplitude electrostatic solitary waves, we transform the set of Eqs. (1)–(4) to a stationary frame moving with velocity V, the solitary wave velocity, i.e., $\xi = (x - Mt)$ where $M = V/C_i$ is the Mach number with respect to the ion thermal velocity. Then, solving for perturbed densities, putting these expressions in the Poisson equation, and assuming appropriate boundary conditions for the localized disturbances along with the conditions that $\phi = 0$, and $d\phi/d\xi = 0$ at $\xi \to \pm, \infty$, we get the following energy integral,

$$\frac{1}{2}\left(\frac{\partial\phi}{\partial\xi}\right)^2 + \psi(\phi, M) = 0, \tag{5}$$

where

$$\begin{aligned}
\psi(\phi, M) = {} & \mu n_c^0\left\{(M - v_c)^2 - \frac{(M - v_c)}{\sqrt{2}}B_c^{1/2}\right\} \\
& + n_c^0 T_c\left\{1 - 2\sqrt{2}(M - v_c)^3 B_c^{-3/2}\right\} \\
& + \mu n_1^0\left\{(M - v_1)^2 - \frac{(M - v_1)}{\sqrt{2}}B_1^{1/2}\right\} \\
& + n_1^0 T_1\left\{1 - 2\sqrt{2}(M - v_1)^3 B_1^{-3/2}\right\} \\
& + \mu n_2^0\left\{(M - v_2)^2 - \frac{(M - v_2)}{\sqrt{2}}B_2^{1/2}\right\} \\
& + n_2^0 T_2\left\{1 - 2\sqrt{2}(M - v_2)^3 B_2^{-3/2}\right\} \\
& + n_i^0\left\{(M - v_i)^2 - \frac{(M - v_i)}{\sqrt{2}}B_i^{1/2}\right\} \\
& + n_i^0\left\{1 - 2\sqrt{2}(M - v_i)^3 B_i^{-3/2}\right\},
\end{aligned} \tag{6}$$

is the pseudopotential, also known as the Sagdeev potential. Here,

$$\begin{aligned}
B_c &= A_c \pm \sqrt{A_c^2 - \frac{12T_c(M - v_c)^2}{\mu}}, \\
B_1 &= A_1 \pm \sqrt{A_1^2 - \frac{12T_1(M - v_1)^2}{\mu}}, \\
B_2 &= A_2 \pm \sqrt{A_2^2 - \frac{12T_2(M - v_2)^2}{\mu}}, \\
B_i &= A_i \pm \sqrt{A_i^2 - 12(M - v_i)^2}, \\
A_c &= (M - v_c)^2 + \frac{3T_c}{\mu} + \frac{2\phi}{\mu}, \\
A_1 &= (M - v_1)^2 + \frac{3T_1}{\mu} + \frac{2\phi}{\mu}, \\
A_2 &= (M - v_2)^2 + \frac{3T_2}{\mu} + \frac{2\phi}{\mu}, \\
A_i &= (M - v_i)^2 + 3 - 2\phi, \mu = \frac{m_e}{m_i}.
\end{aligned} \tag{7}$$

In Eq. (6), $n_j^0 = N_j/N_i$ such that $n_c^0 + n_1^0 + n_2^0 = n_i^0 = 1$, and the temperatures of the species are normalized with the ion temperature. In order that various B_js, which are proportional to the square of the density of the respective jth species, are real and the associated densities attain their undisturbed values in the limit of $\phi \to 0$ when $\xi \to \pm\infty$, we must use the + (plus) sign when the condition $(M - v_j)^2 + \frac{2\phi}{\mu} > \frac{3T_j}{\mu}$ is satisfied, and the – (minus) sign when $(M - v_j)^2 + \frac{2\phi}{\mu} < \frac{3T_j}{\mu}$ holds (Verheest et al., 2008; Lakhina et al., 2009). Further, it is interesting to note that Eq. (5) describes the motion of a pseudo-particle of unit mass in a pseudo-potential ψ where ϕ and ξ play the role of displacement x from the equilibrium and time, respectively.

3. Soliton and double layer solutions

Eq. (5) will give a soliton solution when the pseudo-particle is reflected in the pseudo-potential field and returns to its initial state (zero potential drop). Therefore, for soliton solutions, Sagdeev potential $\psi(\phi, M)$ must satisfy the following conditions:

$$\begin{aligned}
&\psi(\phi, M) = 0, \quad d\psi(\phi, M)/d\phi = 0, \\
&d^2\psi(\phi, M)/d\phi^2 < 0 \quad \text{at } \phi = 0, \\
&\psi(\phi, M) = 0 \quad \text{at } \phi = \phi_0, \quad \text{and} \\
&\psi(\phi, M) < 0 \quad \text{for } 0 < |\phi| < |\phi_0|.
\end{aligned} \tag{8}$$

Double layer solutions could also exist at an upper limit on the Mach number $M = M_{DL}$ provided one more additional condition given below is satisfied,

$$\frac{d\psi(\phi, M)}{d\phi}\Big|_{\phi=\phi_{DL}, M=M_{DL}} = 0 \tag{9}$$

When the conditions given by Eqs. (8) and (9) are satisfied, the pseudo-particle is not reflected at $\phi = \phi_{DL}$ because of the vanishing pseudo-force and pseudo-velocities. Instead, it goes to another state producing an asymmetrical double layer (DL) with a net potential drop of ϕ_{DL}, where ϕ_{DL} is the amplitude of the double layer.

From Eqs. (6) and (8), it is seen that $\psi(\phi, M)$ and its first derivative with respect to ϕ vanish at $\phi = 0$. The condition $d^2\psi(\phi, M)/d\phi^2 < 0$ at $\phi = 0$ is satisfied provided $M > M_0$, where M_0 satisfies the equation

$$\begin{aligned}
f(M_0) \equiv {} & \frac{n_c^0}{\mu\left[(M_0 - v_c)^2 - \frac{3T_c}{\mu}\right]} + \frac{n_1^0}{\mu\left[(M_0 - v_1)^2 - \frac{3T_1}{\mu}\right]} \\
& + \frac{n_2^0}{\mu\left[(M_0 - v_2)^2 - \frac{3T_2}{\mu}\right]} + \frac{n_i^0}{\left[(M_0 - v_i)^2 - 3\right]} = 0.
\end{aligned} \tag{10}$$

Eq. (10) yields 6 roots but all the roots will not be physical. We will consider here only the real positive roots for M_0, or the critical Mach numbers. For $M_0 \leqslant (3T_c/\mu)^{1/2}$, the Langmuir modes can be ruled out as the phase velocity of the Langmuir wave always exceeds the thermal speed of the hot (core) electron component. For such a case, only the ion- and electron-acoustic modes can exist. Since an analytical solution of Eq. (10) for the general case of counterstreaming electron beam is not possible, we consider some limiting cases. On putting all the drift speeds to zero, i.e., $v_c = v_1 = v_2 = v_i = 0$, and considering $N_1 = N_2 = N_B$ and $T_1 = T_2 = T_B$, Eq. (10) yields two values of positive Mach numbers, namely,

$$M_{ia} \approx [3 + (3T_c/n_c^0)/(1 + 2N_BT_c/N_cT_B)]^{1/2}, \tag{11}$$

and

$$M_{ea} \approx (2N_B/N_i)^{1/2}(3T_c/\mu)^{1/2}[1 + N_cT_B/2N_BT_c)]^{1/2}, \tag{12}$$

which we can identify with the ion-acoustic and electron-acoustic modes, respectively. For the case of identical electron beams streaming in the same directions, i.e., $v_c = v_i = 0$, and $v_1 = v_2 = v_B$, the critical Mach number for ion-acoustic mode is not much affected by the electron beams and is still approximately described by Eq. (11). The positive critical Mach number for the electron-acoustic mode is modified by the electron beams, and for $N_B \ll N_c$, can be expressed approximately by,

$$M_{eaB} \approx v_B + (2N_B/N_c)^{1/2}(3T_c/\mu)^{1/2}. \tag{13}$$

Eq. (13) shows that the presence of electron beam can either increase or decrease the critical Mach number of the electron-acoustic modes provided $v_B > 0$ or $v_B < 0$, respectively. Therefore, for the case of counterstreaming electron beams, we expect two critical Mach numbers for the electron-acoustic modes, i.e., the one with the lower value associated with $v_B < 0$, and the other with the higher value associated with $v_B > 0$ electron beam.

The numerical solution of Eq. (10) indeed yields three critical positive Mach numbers which we tentatively identify as an ion-acoustic (lowest M_0), slow electron-acoustic (intermediate M_0) and fast electron-acoustic (highest M_0) beam modes. However, for a given set of plasma parameters, any one, two or all the three modes can satisfy the soliton conditions given above.

4. Numerical results

We have numerically solved Eq. (6) for the Sagdeev potential, $\psi(\phi, M)$, as a function of ϕ for various values of Mach numbers for the case of counterstreaming electron beams having equal densities (i.e., $N_1 = N_2 = N_B$) and temperature (i.e., $T_1 = T_2 = T_B$), and equal and opposite streaming velocities (i.e., $v_1 = -v_2 = v_B$). Results are shown for some typical plasma parameters in Fig. 1(a)–(c) for the counterstreaming electron beam velocity $v_B = 1.0$. Here, and in all the figures and tables, we have taken core electron drift velocity, $v_c = 0$ and ion beam velcoity, $v_i = 0$. The solitary wave solutions of three types, which we tentatively call as ion-acoustic (with lowest M_0), slow electron-acoustic (with intermediate M_0, and fast electron-acoustic modes (with largest M_0), are found when the Mach numbers exceed the critical values given by the solution of Eq. (10).

Fig. 1(a) shows that the ion-acoustic solitons have positive potentials. The maximum electrostatic potential ϕ_0 increases with the increase of the Mach number, M, as seen from curves 1 and 2. For curve 3, the soliton solution does not exist. Hence there is an upper value for M, say M_{max}, above which soliton solutions do not exist. This is true for ion-acoustic as well as for slow and fast electron-acoustic solitary structures. Fig. 1(b) shows that for the same plasma parameters, but for higher values of the Mach number, M, slow electron-acoustic solitons can exist. However, the slow electron-acoustic solitons have negative potentials.

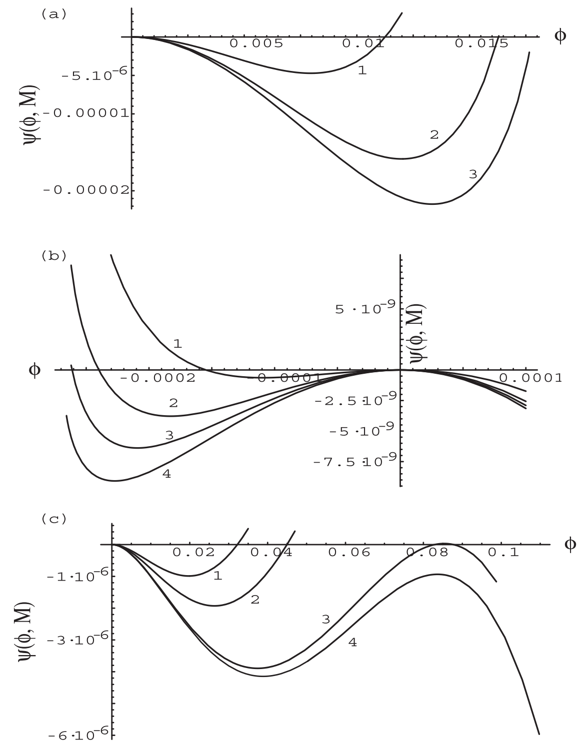

Fig. 1. Sagdeev potential, $\psi(\phi, M)$ versus potential ϕ for various values of Mach numbers for the case of identical (equal density, temperature, and equal and opposite streaming velocity) counterstreaming electron beams. The normalized plasma parameters are $N_c/N_i = 0.5$, $N_1/N_i = N_2/N_i = N_B/N_i = 0.25$, $v_c = v_i = 0.0$, $v_1/C_i = -v_2/C_i = v_{B/C_i} = 1.0$, $T_c/T_i = 0.5$, $T_1/T_i = T_2/T_i = T_B/T_i = 0.1$. (a) (Top panel) is for ion-acoustic solitary waves, and for Mach number $M = 1.9$, 1.915 and 1.92 for the curves 1, 2, and 3, respectively. The soliton solution does not exist for M equal or exceeding the value for the curve 3. (b) (Middle panel) corresponds to slow electron-acoustic solitons, and for $M = 23.44$, 23.45, 23.454 and 23.457 for the curves 1, 2, 3, and 4, respectively. The soliton solution does not exist for $M \geqslant 23.457$ (curve 4). (c) (Bottom panel) shows fast electron-acoustic solitons/double layer for the Mach number $M = 40.850$, 40.8850, 40.9262 and 40.93 for the curves 1, 2, 3 and 4, respectively. The curve 3 corresponds to the double layer solution. The double layer/soliton solution does not exist for $M \geqslant 40.93$ (curve 4).

In this case also the maximum electrostatic potential ϕ_0 increases with an increase in M (see curves 1, 2 and 3 of Fig. 1(b)). For curve 4, the soliton solution does not exist. Fig. 1(c) shows that for the same plasma parameters, but for still higher values of the Mach number, M, fast electron-acoustic solitons can exist. In contrast to the slow electron-acoustic case, the fast electron-acoustic solitons have positive potentials (cf. curves 1, 2, and 3 of Fig. 1(c)). It is interesting to note that curve 3 satisfies the double layer condition given by Eq. (9). Therefore the curve 3 corresponds to the double layer solution. Once again, the maximum electrostatic potential ϕ_0 increases with an increase in M as is evident from curves 1, 2, and 3. For curve 4, the soliton/double layer solution does not exist.

It is, therefore, clear that the Sagdeev potential analysis gives the upper limit on M, i.e., M_{max}, for the soliton solutions. When Eq. (9) is also satisfied, M_{max} simply equals M_{DL}, thus supporting a double layer solution. For $M > M_{max}$

or $M > M_{DL}$ no soliton or double layer can exist as at least one B_j no longer remains real leading to an unphysical situation where the species densities become complex. We carried out Sagdeev potential analysis for various values of the plasma parameters. The range of Mach numbers for which ion-, and slow and fast electron-acoustic solitons (double layers) exist, i.e., $M_0 < M \leqslant M_{max}(M_{DL})$, are given in Tables 1–4. The range of potentials associated with these solitary

Table 1
Properties of ion-acoustic, slow electron-acoustic and fast electron-acoustic solitons for different values of the normalized core electron density, (N_c/N_i), and beam electron density (N_B/N_i), for the case of equal density and temperature, but equal and opposite streaming velocity electron beams with $v_{B/C_i} = 1.0$, $T_B/T_i = 0.1$, and $T_c/T_i = 0.5$. Here as well as in all other tables $v_c = v_i = 0.0$.

Normalized electron densities N_c, N_B	Ion-acoustic solitons		Slow electron-acoustic solitons		Fast electron-acoustic solitons	
	Range of Mach number $M_0 < M \leqslant M_{max}$	Range of potential ϕ	Range of Mach number $M_0 < M \leqslant M_{max}$	Range of potential ϕ	Range of Mach number $M_0 < M \leqslant M_{max}$	Range of potential ϕ
0.7, 0.15	1.918–1.985	0.001–0.032	23.399–23.441	−0.0001 to −0.0028	34.880–36.195	−0.01 to −0.038
0.6, 0.2	1.891–1.947	0.001–0.023	23.416–23.450	−0.0001 to −0.00026	37.892–38.352	−0.01 to −0.052
0.5, 0.25	1.870–1.915	0.001–0.016	23.426–23.454	−0.0001 to −0.00026	40.685–40.9262	0.01–0.085 (DL)
0.3, 0.35	1.842–1.878	0.001–0.01	23.440–23.455	−0.0001 to −0.00024	45.767–48.95	0.01–0.097
0.1, 0.45	1.824–1.850	0.0005–0.0066	23.445–23.4615	−0.0001 to −0.00026	50.341–52.00	0.001–0.0084

Table 2
Properties of ion-acoustic, slow electron-acoustic and fast electron-acoustic solitons for different values of the normalized beam streaming velocity, v_B/C_i, for the case of counter-streaming electron beams with $N_c/N_i = 0.5$ and $N_B/N_i = 0.25$, $T_B/T_i = 0.1$, and $T_c/T_i = 0.5$.

Normalized electron beam velocity v_B/C_i	Ion-acoustic solitons		Slow electron-acoustic solitons		Fast electron-acoustic solitons	
	Range of Mach number $M_0 < M \leqslant M_{max}$	Range of potential ϕ	Range of Mach number $M_0 < M \leqslant M_{max}$	Range of potential ϕ	Range of Mach number $M_0 < M \leqslant M_{max}$	Range of potential ϕ
0.0	1.871–1.915	0.001–0.0163	–	–	40.660–40.9027	0.01–0.085 (DL)
1.0	1.869–1.915	0.001–0.0163	23.427–23.454	−0.0001 to −0.00026	40.685–40.9262	0.01–0.0835 (DL)
5.0	–	–	22.450–22.900	−0.001 to −0.0051	41.390–41.4953	0.01–0.058 (DL)
10.0	–	–	19.683–21.050	−0.001 to −0.0156	–	–
20.0	–	–	–	–	48.045–48.0463	−0.0004 to −0.0014 (Noisy DL)

Table 3
Properties of ion-acoustic, slow electron-acoustic and fast electron-acoustic solitons for different values of the normalized electron beam temperature, T_B/T_i, for the case of counter-streaming electron beams with $N_c/N_i = 0.5$, $N_B/N_i = 0.25$, $v_B/C_i = 1.0$, and $T_c/T_i = 0.5$.

Normalized electron beam temperature T_B/T_i	Ion-acoustic solitons		Slow electron-acoustic solitons		Fast electron-acoustic solitons	
	Range of Mach number $M_0 < M \leqslant M_{max}$	Range of potential ϕ	Range of Mach number $M_0 < M \leqslant M_{max}$	Range of potential ϕ	Range of Mach number $M_0 < M \leqslant M_{max}$	Range of potential ϕ
0.3	2.030–2.139	0.01–0.083	40.565–40.615	−0.00005 to −0.00025	47.018–47.03421	0.001–0.01175 (DL)
0.2	1.963–2.025	0.005–0.038	33.135–33.170	−0.00005 to −0.00026	43.957–44.0546	0.001–0.04 (DL)
0.1	1.869–1.915	0.001–0.0163	23.427–23.454	−0.0001 to −0.000262	40.685–40.9262	0.01–0.0835 (DL)
0.05	1.808–1.83	0.001–0.0045	16.552–16.580	−0.00005 to −0.0002625	38.952–39.2999	0.01–0.1185 (DL)
0.02	1.764–1.7745	0.0001–0.000898	10.441–10.475	−0.00005 to −0.000258	37.874–38.303	0.01–0.1435

Table 4
Properties of ion-acoustic, slow electron-acoustic and fast electron-acoustic solitons for different values of the normalized core electron temperature, T_{ce}/T_i, for the case of counter-streaming electron beams with $N_c/N_i = 0.5$, $N_B/N_i = 0.25$, $v_B/C_i = 1.0$, and $T_B/T_i = 0.3$.

Normalized core electron temperature T_c/T_i	Ion-acoustic solitons		Slow electron-acoustic solitons		Fast electron-acoustic solitons	
	Range of Mach number $M_0 < M \leqslant M_{max}$	Range of potential ϕ	Range of Mach number $M_0 < M \leqslant M_{max}$	Range of potential ϕ	Range of Mach number $M_0 < M \leqslant M_{max}$	Range of potential ϕ
10.0	2.178–2.350	0.01–0.187	40.636–40.645	−0.00005 to −0.000269	168.468–170.4655	0.1–2.85 (DL)
5.0	2.167–2.30	0.01–0.144	40.635–40.645	−0.00005 to −0.000269	120.848–122.125	0.1–1.3 (DL)
1.0	2.094–2.225	0.01–0.120	40.616–40.635	−0.0001 to −0.000244	59.866–60.09945	0.01–0.122 (DL)
0.5	2.031–2.135	0.001–0.081	40.565–40.615	−0.00005 to −0.00025	47.018–47.0342	0.001–0.01175 (DL)

structures are also given in Tables 1–4. When the double layer solution exists, it is mentioned as "DL" along with the potential range.

Fig. 2 shows the variation of Sagdeev potential versus the potential ϕ for different values of counterstreaming electron beam velocity v_B and a given Mach number and fixed plasma parameters. Fig. 2(a)(top panel) is for the ion-acoustic solitons for $M = 2.05$, and $v_B = 1.0$, 1.5 and 2.0 for the curves 1, 2 and 3, respectively. The solitons have positive potential and their maximum amplitude tends to increase slightly with increasing v_B. The soliton solutions exist for $0 \leqslant v_{B/C_i} \leqslant 2.049$. Fig. 2(b)(middle panel) is for the slow electron-acoustic solitons for $M = 40.578$, and $v_B = 1.0$, 1.2 and 1.4 for the curves 1, 2 and 3, respectively. The slow electron-acoustic solitons have negative potential and their maximum amplitude tends to increase with increasing v_B. The soliton solutions occur for $0.93 \leqslant v_{B/C_i} \leqslant 1.434$. Fig. 2(c)(bottom panel) shows the fast electron-acoustic solitons for $M = 47.0342$, and $v_B = 1.0$, 1.025, 1.05, and 1.075 for the curves 1, 2, 3 and 4, respectively. The fast electron-acoustic solitons/double layer have positive potential, and their maximum amplitude tends to decrease with increasing v_B. The curve 1 is for the double layer. However, the double layer/soliton solutions exist in the range of $1.0 \leqslant v_B/C_i \leqslant 1.097$.

In Fig. 3, we show variation of Sagdeev potential with ϕ for various values of the beam temperature, T_B when the Mach number and other plasma parameters are fixed. Fig. 3(a)(top panel) shows the ion-acoustic solitons for $M = 2.05$, and $T_B = 0.3$, 0.275 and 0.25 for the curves 1, 2 and 3, respectively. The solitons have positive potentials and their maximum amplitude tends to increase with decreasing T_B (cf. curves 1, 2 and 3). Soliton solutions exist for $0.206 \leqslant T_B/T_i \leqslant 0.335$. Fig. 3(b)(middle panel) shows the slow electron-acoustic solitons for $M = 40.578$, and $T_B = 0.3$, 0.2999 and 0.2995 for the curves 1, 2 and 3, respectively. The solitons have negative potential and their maximum amplitude tends to increase with decreasing T_B (cf. curves 1, 2 and 3). Soliton solutions occur in the range of $0.2995 \leqslant T_B/T_i \leqslant 0.30012$. Fig. 3(c)(bottom panel) is for fast electron-acoustic solitons for $M = 47.025$, and $T_B = 0.3$, 0.2999 and 0.2997 for the curves 1, 2 and 3, respectively. The solitons have positive potential and their maximum amplitude tends to increase with decreasing T_B

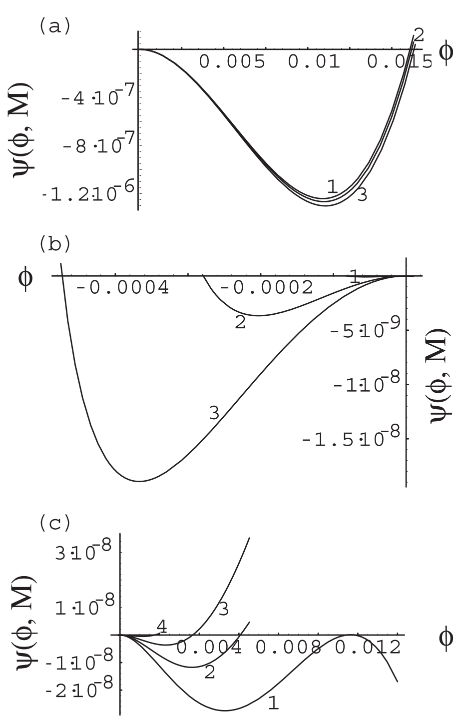

Fig. 2. Sagdeev potential, $\psi(\phi, M)$ versus potential ϕ for various values of the normalized counter-streaming electron beam speed v_{B/C_i} for the same plasma parameters as in Fig. 1 except that $T_B/T_i = 0.3$ instead of 0.1. (a) (Top panel) shows ion-acoustic solitary waves for Mach number $M = 2.05$, and $v_{B/C_i} = 1.0$, 1.5 and 2.0 for the curves 1, 2, and 3, respectively. The soliton solutions exist for $0 \leqslant v_{B/C_i} \leqslant 2.049$. (b) (Middle panel) corresponds to slow electron-acoustic solitons, for $M = 40.578$ and for $v_{B/C_i} = 1.0$, 1.2 and 1.4 for the curves 1, 2, and 3, respectively. The soliton solutions exist for $0.93 \leqslant v_{B/C_i} \leqslant 1.434$. (c) (Bottom panel) shows fast electron-acoustic solitons/double layer for the Mach number $M = 47.0342$ and $v_{B/C_i} = 1.0$, 1.025, 1.05, and 1.075 for the curves 1, 2, 3, and 4, respectively. The curve 1 corresponds to the double layer solution. The double layer/soliton solutions exist for $1 \leqslant v_{B/C_i} \leqslant 1.097$.

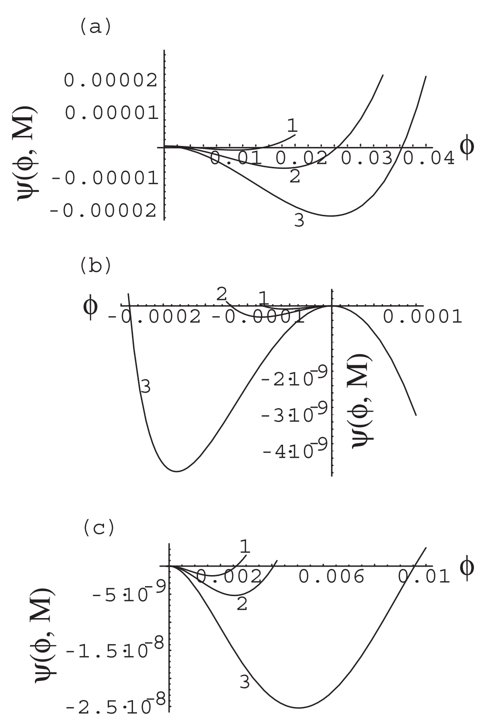

Fig. 3. Variation of Sagdeev potential with $\psi(\phi, M)$ versus potential ϕ for various values of electron beam temperature T_B/T_i for the same plasma parameters as in Fig. 1. (a) (Top panel) shows ion-acoustic solitary waves for Mach number $M = 2.05$, and $T_B/T_i = 0.3$, 0.275 and 0.25 for the curves 1, 2, and 3, respectively. The soliton solutions exist for $0.206 \leqslant T_B/T_i \leqslant 0.335$. (b) (Middle panel) corresponds to slow electron-acoustic solitons, for $M = 40.578$ and for $T_B/T_i = 0.3$, 0.2999 and 0.2995 for the curves 1, 2, and 3, respectively. The soliton solutions exist for $0.2995 \leqslant T_B/T_i < 0.30012$. (c) (Bottom panel) shows fast electron-acoustic solitons/double layer for the Mach number $M = 47.025$ and $T_B/T_i = 0.3$, 0.2999 and 0.2997 for the curves 1, 2, and 3, respectively. The soliton solutions exist for $0.2997 \leqslant T_B/T_i \leqslant 0.30022$.

(cf. curves 1, 2 and 3). Soliton solutions exist for $0.2997 \leqslant T_B/T_i \leqslant 0.30022$.

From Figs. 2 and 3, it is clear that for a given Mach number, all the three type of solitons can exist in a narrow range of beam electron parameters like counter-streaming velocity, v_B, beam temperature, T_B and beam density, N_B (not shown). The ranges of Mach numbers and potentials for variations with other plasma parameters are given in Tables 1–4.

Table 1 illustrates the properties of the ion-acoustic, slow electron-acoustic and fast electron-acoustic solitons when the core electron density, N_c, and beam density, N_B, for equal counterstreaming electron beam is varied. The ion-acoustic solitons have positive potentials (column 3), the slow electron-acoustic solitons have negative potential (column 5), and fast electron-acoustic solitons have first negative potentials and then change over to positive potential double layer and solitons (column 7) as the core (beam) electron density is decreased (increased). Both the Mach numbers and the potential amplitude for the ion-acoustic solitons decrease with the decrease of core electron density. For the slow electron-acoustic solitons, the Mach numbers tend to increase and the potential amplitudes first tend to decrease and then increase as N_c is decreased. On the other hand, for the fast electron-acoustic solitons, the Mach number tend to increase and the potential amplitudes first increases and then decrease as N_c is decreased.

Table 2 summarizes the properties of the ion-acoustic, slow electron-acoustic and fast electron-acoustic solitons for various values of the beam velocity v_B/C_i. It is interesting to note that positive potential ion-acoustic solitons do not exist for $v_B/C_i \geqslant 5.0$ (cf. columns 2–3). The negative potential slow electron-acoustic solitons do not exist for $v_B/C_i = 0.0$ and $v_B/C_i \geqslant 20.0$ (columns 4–5). The fast electron-acoustic solitons/double layers have positive potentials at low beam velocities and disappear at $v_B/C_i = 10.0$ and then reappear with negative potentials when $v_B/C_i \geqslant 20.0$ (cf. columns 6–7).

Table 3 clearly shows that the range of Mach number, M for all the three type of modes gets lowered as the beam temperature, T_B/T_i, is decreased (see columns 2, 4 and 6). The amplitude of the positive potential ion-acoustic solitons decreases as T_B/T_i decreases (column 3). The amplitude of negative potential slow electron-acoustic solitons is not much affected by the variations in T_B/T_i (column 5). The fast electro-acoustic solitons/double layers have positive potentials at $T_B/T_i = 0.3$, which increase as T_B/T_i is decreased (column 7). For $T_B/T_i \leqslant 0.02$, only fast electron-acoustic solitons are found.

Table 4 illustrates that the range of Mach number, M for all the three type of modes gets lowered as the core electron temperature, T_c/T_i, is decreased from 10.0 to 0.1 (columns 1, 2, 4 and 6). The amplitudes of the positive potential ion-acoustic solitons decrease as T_c/T_i decreases (column 3). The amplitudes of negative potential slow electron-acoustic soltitons are not much affected when T_c/T_i decreases from 10.0 to 0.5 (column 5). The amplitude of fast electron-acoustic solitons/double layers decreases as T_c/T_i is decrease from 10.0 to 0.5 (column 7).

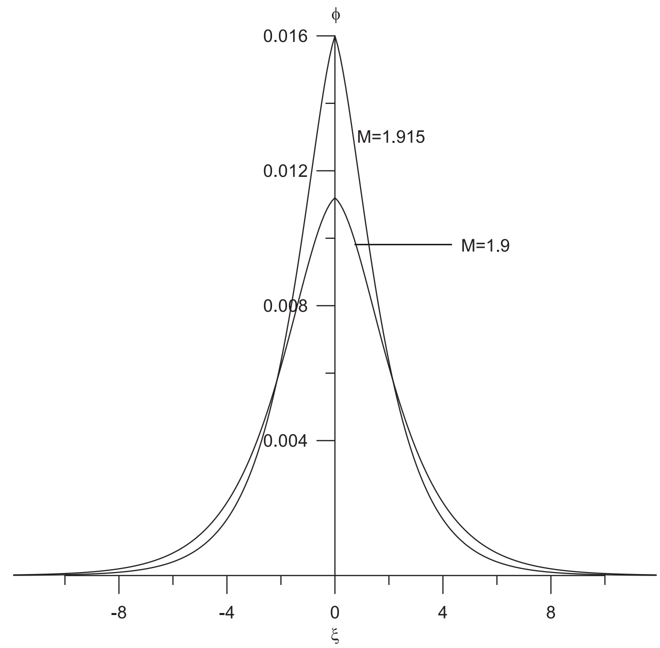

Fig. 4. Variation of electrostatic potential ϕ versus ξ for the ion-acoustic solitons for different values of the Mach number, M, for the parameters of Fig. 1a.

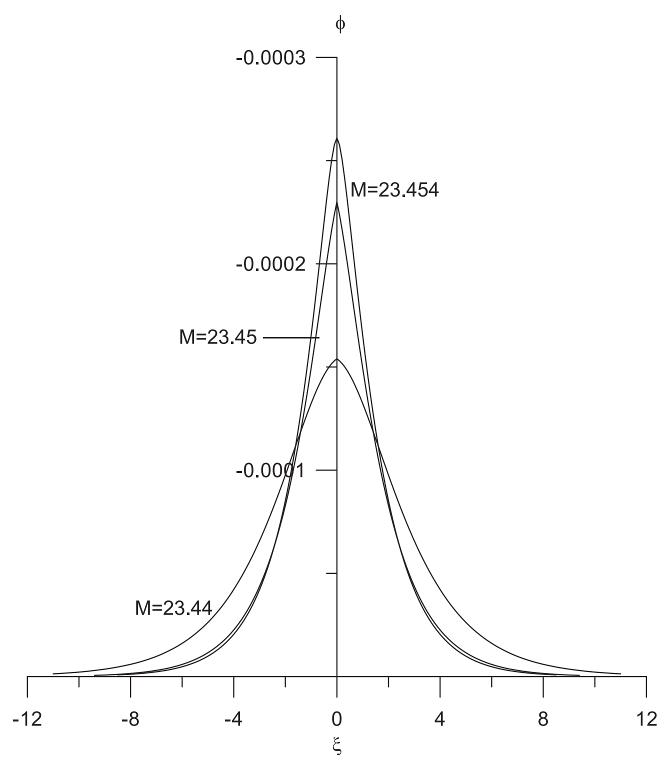

Fig. 5. Variation of electrostatic potential ϕ versus ξ for the slow electron-acoustic solitons for different values of the Mach number, M, for the parameters of Fig. 1b.

Figs. 4–6 show the variations of potential amplitude, ϕ, versus ξ for ion-acoustic, slow electron-acoustic and fast electron-acoustic solitons, respectively, for different values of the Mach numbers, M, for the parameters of Fig. 1. It is clear that soliton amplitudes for ion-acoustic (Fig. 4), slow electron-acoustic (Fig. 5) and fast electron-acoustic solitons increase as M increases. For the case of fast electron-acoustic mode, at the maximum value of the Mach number we have double layer (cf. Fig. 6).

Fig. 7 shows the electric field E profiles for the fast electron-acoustic solitons and double layer corresponding to potential profiles shown in Fig. 6. The solitons have bipolar electric fields whereas the double layer has a monopolar electric field structure.

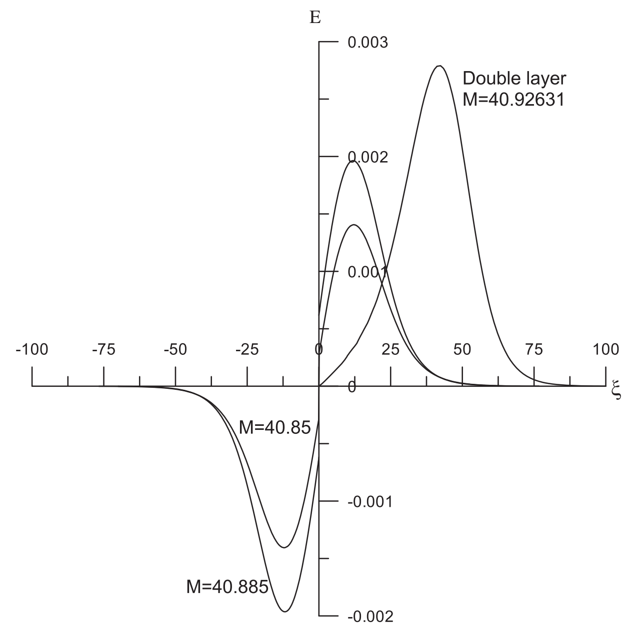

Fig. 7. Electric field, E, profiles for the fast electron-acoustic solitons and double layer for the parameters of Fig. 1c. The electric field has bipolar structure for the solitons and a monopolar structure for the double layer.

5. Discussion

We studied large amplitude ion- and electron-acoustic solitary waves in an unmagnetized four component plasma consisting of core electrons, counterstreaming electron beams and one type of ion population (Lakhina et al., 2009). The model treats all the species as mobile, and in principle all species can have an arbitrary beam velocity. We have specialized to the case of identical (equal density, N_B, and temperature, T_B) counterstreaming electron beams having equal and opposite streaming velocity, v_B. The effects of the variation of N_B, T_B, v_B, and core electron density, N_c and temperature, T_{ce} on the properties of ion- and electron-acoustic solitons/double layer are investigated numerically. In general, the model predicts the existence of ion-acoustic, slow and fast electron-acoustic modes. Depending upon the plasma parameters, either only one, two or all the three modes can coexist in different and distinct Mach number regime. For example, if the beam velocity is zero, i.e., $v_B = 0.0$, only two types of solutions, namely, the ion-acoustic and the electron-acoustic solitons/double layers, are possible (cf. Table 2). For finite beam velocity, i.e., $v_B \neq 0.0$, three types of solutions, namely, ion-acoustic, slow and fast electron-acoustic soliton/double layer, are possible. We have presented numerical results for the cases where the core electrons and the ions have no beams component, i.e., $v_c = v_i = 0.0$.

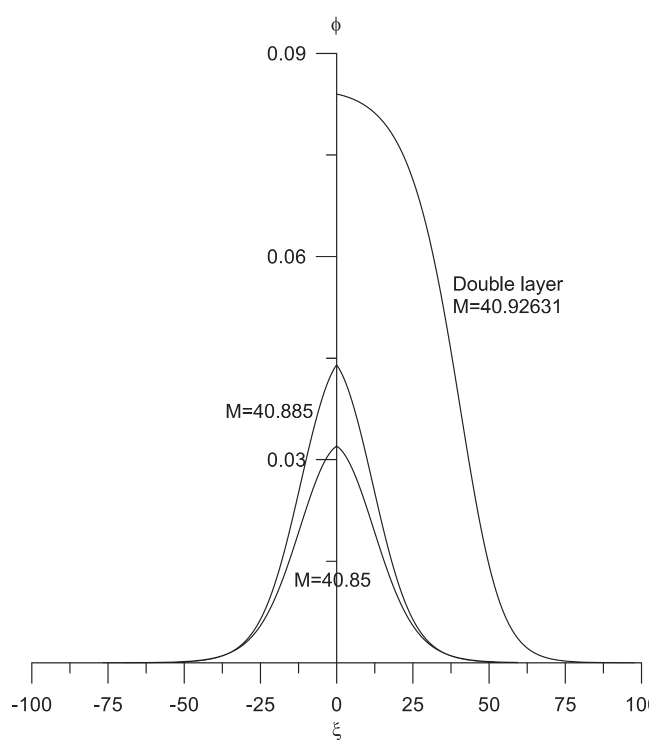

Fig. 6. Variation of electrostatic potential ϕ versus ξ for the fast electron-acoustic solitons (Mach numbers, $M = 40.85$ and 40.885) and double layer ($M = 40.92631$) for the parameters of Fig. 1c.

For identical counter-streaming electron beams, and plasma parametric survey done here, generally, the ion acoustic solitons have positive potentials, slow-electron acoustic solitons have negative potentials and fast electron-acoustic solitons and double layers have positive potentials for $N_c/N_i \leqslant 0.5$ and negative potential for $N_c/N_i \geqslant 0.6$. As beam speed is increased, first ion-acoustic and then slow electron-acoustic solitons disappear. At large beam speed, only electron-acoustic solitons/double layers survive. For a fixed Mach number, a decrease in beam temperature tends to increase the soliton amplitudes.

Decreasing core electron temperatures tend to result in decreased amplitudes for all the three modes.

Applications of this models to ESWs observed in some regions of the magnetosphere, e.g., near bow shock, in auroral/cusp region, plasma sheet boundary layer, etc. are being looked into, and the results will be reported elsewhere.

Acknowledgement

GSL would like to thank the Indian National Science Academy, New Delhi, India, for the support under the Senior Scientist scheme.

References

Åsnes, A., Taylor, M.G.G.T., Borg, A.L., Lavraud, B., Friedel, R.W.H., Escoubet, C.P., Laakso, H., Daly, P., Fazakerley, A.N. Multispacecraft observation of electron beam in reconnection region. J. Geophys. Res. 113, A07S30, doi:10.1029/2007JA012770, 2008.

Bale, S.D., Kellogg, P.J., Larsen, D.E., Lin, R.P., Goetz, K., Lepping, R.P. Bipolar electrostatic structures in the shock transition region: evidence of electron phase space holes. Geophys. Res. Lett. 25, 2929–2932, 1998.

Berthomier, M., Pottellette, R., Malingre, M., Khotyaintsev, Y. Electron-acoustic solitons in an electron-beam plasma system. Phys. Plasmas 7, 2987, 2000.

Berthomier, M., Pottelette, R., Muschietti, L., Roth, I., Carlson, C.W. Scaling of 3D solitary waves observed by FAST and POLAR. Geophys. Res. Lett. 30, 2148, 2003.

Bostrom, R., Gustafsson, G., Holback, G., Holmgren, G., Koskinen, H., Kintner, P. Characteristics of solitary waves and weak double layers in the magnetospheric plasma. Phys. Rev. Lett. 61, 82, 1988.

Bounds, S.R., Pfaff, R.F., Knowlton, S.F., Mozer, F.S., Temerin, M.A., Kletzing, C.A. Solitary potential structures associated with ion and electron beams near 1 R_E altitude. J. Geophys. Res. 104, 28709, 1999.

Cattell, C., Dombeck, J., Wygant, J.R., Hudson, M.K., Mozer, F.S. Comparisions of polar satellite observations of solitary wave velocities in the plasma sheet boundary and the high altitude cusp to those in the auroral zone. Geophys. Res. Lett. 26, 425–428, 1999.

Dubouloz, N., Pottellette, R., Malingre, M., Holmgren, G., Lindqvist, P.A. Detailed analysis of broadband electrostatic noise in the dayside auroral zone. J. Geophys. Res. 96, 3565, 1991a.

Dubouloz, N., Pottelette, R., Malingre, M., Treumann, R.A. Generation of broadband electrostatic noise by electron acoustic solitons. Geophys. Res. Lett. 18, 155, 1991b.

Dubouloz, N., Treumann, R.A., Pottelette, R., Malingre, M. Turbulence generated by a gas of electron acoustic solitons. J. Geophys. Res. 98, 17415, 1993.

El-Taibany, W.F. Electron-acoustic solitary waves and double layers with an electron beam and phase space electron vortices in space plasmas. J. Geophys. Res. 110, A01213, doi:10.1029/2004JA010525, 2005.

Ergun, R.E., Calrson, C.W., McFadden, J.P., Mozer, F.S., Delory, D.T., et al. FAST satellite observations of large-amplitude solitary structures. Geophys. Res. Lett. 25, 2041–2044, 1998.

Deng, X.H., Tang, R.X., Matsumoto, H., Pickett, J.S., Fazakerley, A., et al. Observations of electrostatic solitary waves associated with reconnection by Geotail and Cluster. Adv. Space Res. 37, 1373–1381, doi:10.1016/j.asr.2005.05.129, 2006.

Franz, J.R., Kintner, P.M., Pickett, J.S. Polar observation of coherent electric field structures. Geophys. Res. Lett. 25, 1277–1280, 1998.

Fujimoto, M., Sugiyama, T., Mukai, T., Saito, Y., Yamamoto, T., Kokubun, S. Highly collimated electron beams in the dawn-flank of the magnetotail. Phys. Chem. Earth 22, 645–651, 1997.

Ghosh, S.S., Pickett, J.S., Lakhina, G.S., Winningham, J.D., Lavraud, B., Décréau, P.M.E. Parametric analysis of positive amplitude electron acoustic solitary waves in a magnetized plasma and its application to boundary layers. J. Geophys. Res. 113, A06218, doi:10.1029/2007JA012768, 2008.

Kakad, A.P., Singh, S.V., Reddy, R.V., Lakhina, G.S., Tagare, S.G., Verheest, F. Generation mechanism for electron acoustic solitary waves. Phys. Plasmas 14, 052305, doi:10.1063/1.2732176, 2007.

Kakad, A.P., Singh, S.V., Reddy, R.V., Lakhina, G.S., Tagare, S.G. Electron acoustic solitary waves in the Earth's magnetotail region. Adv. Space Res. 43, 1945–1949, 2009.

Lakhina, G.S., Tsurutani, B.T., Kojima, H., Matsumoto, H. Broadband plasma waves in the boundary layers. J. Geophys. Res. 105, 27,791–27,831, 2000.

Lakhina, G.S., Tsurutani, B.T., Singh, S.V., Reddy, R.V. Some theoretical models for solitary structures of the boundary layer waves. Nonlinear Process. Geophys. 10, 65, 2003.

Lakhina, G.S., Kakad, A.P., Singh, S.V., Verheest, F. Ion- and electron-acoustic solitons in two-electron temperature space plasmas. Phys. Plasmas 15, 062903, 2008a.

Lakhina, G.S., Singh, S.V., Kakad, A.P., Verheest, F., Bharuthram, R. Study of nonlinear ion- and electron-acoustic waves in multi-component space plasmas. Nonlinear Process. Geophys. 15, 903–913, 2008b.

Lakhina, G.S., Singh, S.V., Kakad, A.P., Goldstein, M.L., Viñas, A.F., Pickett, J.S. A mechanism for electrostatic solitary structures in the Earth's magnetosheath. J. Geophys. Res. 114, A09212, doi:10.1029/2009JA014306, 2009.

Li, S.Y., Deng, X.H., Zhou, M., Tang, R.X., Liu, K., Kojima, H., Matsumoto, H. Statistical study of electrostatic solitary waves associated with reconnection: Geotail observations. Adv. Space Res. 43, 394400, 2009.

Mace, R.L., Baboolal, S., Bharuthram, R., Hellberg, M.A. Arbitrary amplitude electron-acoustic solitons in a two electron-component plasma. J. Plasma Phys. 45, 323, 1991.

Mamun, A.A., Shukla, P.K., Stenflo, L. Obliquely propagating electron-acoustic solitary waves. Phys. Plasmas 9, 1474, 2002.

Matsumoto, H., Kojima, H., Miyatake, T., Omura, Y., Okada, M., et al. Electrostatic solitary waves (ESW) in the magnetotail: BEN wave forms observed by GEOTAIL. Geophys. Res. Lett. 21, 2915, 1994.

McFadden, J.P., Carlson, C.W., Ergun, R.E., Chaston, C.C., Mozer, F.S., Temerin, M., Klumpar, D.M., Shelley, E.G., Peterson, W.K., Moebius, E., Kistler, L., Elphic, R., Strangeway, R., Cattell, C., Pfaff, R. Electron modulation and ion cyclotron waves observed by FAST. Geophys. Res. Lett. 25, 2045–2048, 1998.

Mozer, F.S., Ergun, R.E., Temerin, M., Cattell, C., Dombeck, J., et al. New features of time domain electric field structures in the auroral acceleration region. Phys. Rev. Lett. 79, 1281, 1997.

Omura, Y., Kojima, H., Matsumoto, H. Computer simulation of electrostatic solitary waves: a nonlinear model of broadband electrostatic noise. Geophys. Res. Lett. 21, 2923, 1994.

Omura, Y., Kojima, H., Miki, N., Mukai, T., Matsumoto, H., Anderson, R. Electrostatic solitary waves carried by diffused electron beams observed by the Geotail spacecraft. J. Geophys. Res. 104, 14627, 1999.

Parks, G.K., McCarthy, M., Fitzenreiter, R., Etcheto, J., Anderson, K., Anderson, R., Eastman, T., Frank, L., Gurnett, D., Huang, C., Lin, R., Lui, A.T.Y., Ogilvie, K., Pedersen, A., Reme, H., Williams, D. Particle and field characteristics of the high-latitude plasma sheet boundary layer. J. Geophys. Res. 89, 8885–8906, 1984.

Pickett, J.S., Menietti, J.D., Gurnett, D.A., Tsurutani, B.T., Kintner, P., Klatt, E., Balogh, A. Solitary potential structures observed in the magnetosheath by the Cluster spacecraft. Nonlinear Process. Geophys. 10, 311, 2003.

Pickett, J.S., Chen, L.-J., Kahler, S.W., Santolik, O., Goldstein, M.L., Lavraud, B., Décréau, P.M.E., Kessel, R., Lucek, E., Lakhina, G.S., Tsurutani, B.T., Gurnett, D.A., Cornilleau-Wehrlin, N., Fazakerley, A., Rème, H., Balogh, A. On the generation of solitary waves observed by Cluster in the near-Earth magnetosheath. Nonlinear Process. Geophys. 12, 181–193, 2005.

Pickett, J.S., Chen, L.-J., Santolik, O., Grimald, S., Lavraud, B., Verkhoglyadova, O.P., Tsurutani, B.T., Lefebvre, B., Fazakerley, A., Lakhina, G.S., Ghosh, S.S., Grison, B., Décréau, P.M.E., Gurnett, D.A., Torbert, R., Cornilleau-Wehrlin, N., Dandouras, I., Lucek, E. Electrostatic solitary waves in current layers: from Cluster observations during a super-substorm to beam experiments at the LAPD. Nonlinear Process. Geophys. 16, 431–442, 2009.

Pottelette, R., Malingre, M., Dubouloz, N., Aparicio, B., Lundin, R., Holmgren, G., Marklund, G. High frequency waves in the Cusp/cleft regions. J. Geophys. Res. 95, 5957–5971, 1990.

Pottelette, R., Ergun, R.E., Truemann, R.A., Berthomier, M., Carlson, C.W., et al. Modulated electron-acoustic waves in auroral density cavities: FAST observations. Geophys. Res. Lett. 26, 2629, 1999.

Singh, N. Space-time evolution of electron-beam driven electron holes and their effects on the plasma. Nonlinear Process. Geophys. 10, 53, 2003.

Singh, S.V., Reddy, R.V., Lakhina, G.S. Broadband electrostatic noise due to nonlinear electron-acoustic waves. Adv. Space. Res. 28, 1643–1648, 2001a.

Singh, N., Loo, S.M., Wells, B.E., Lakhina, G.S. Evolution of electron beam generated waves resulting into transverse ion heating and filamentation of the plasma. J. Geophys. Res. 106, 21165, 2001b.

Singh, S.V., Lakhina, G.S. Electron acoustic solitary waves with non-thermal distribution of electrons. Nonlinear Process. Geophys. 11, 275–279, 2004.

Tagare, S.G., Singh, S.V., Reddy, R.V., Lakhina Electron acoustic solitons in the Earths magnetotail. Nonlinear Process. Geophys. 11, 215–218, 2004.

Teste, A., Parks, G.K. Counterstreaming beams and flat-top electron distributions observed with Langmuir, whistler, and compressional alfvenwaves in earths magnetic tail. Phys. Rev. Lett. 102, 075003, 2009.

Temerin, M., Cerny, K., Lotko, W., Mozer, F.S. Observations of double layers and solitary waves in the auroral plasma. Phys. Rev. Lett. 48, 1175, 1982.

Tsurutani, B.T., Arballo, J.K., Lakhina, G.S., Ho, C.M., Buti, B., Pickett, J.S., Gurnett, D.A. Plasma waves in the dayside polar cap boundary layer: bipolar, monopolar electric pulses and whistler mode waves. Geophys. Res. Lett. 25, 4117, 1998.

Verheest, F., Cattaert, T., Hellberg, M. Compressive and rarefactive electron-acoustic solitons and double layers in space plasmas. Space Sci. Rev. 121, 299–311, 2005.

Verheest, F., Hellberg, M.A., Kourakis, I. Acoustic solitary waves in dusty and/or multi-ion plasmas with cold, adiabatic, and hot constituents. Phys. Plasmas 15, 112309, doi:10.1063/1.3026716, 2008.